International Journal For Recent Developments in Science & Technology
2581-4575
Crossref
A Peer Reviewed Research Journal

HALL EFFECTS ON STEADY MHD LAMINAR FLOW OF VISCO-ELASTIC FLUID EMBEDDED IN POROUS MEDIUM THROUGH A CIRCULAR CYLINDER

M. LOKANADHAM[1], R. SHIVAPRASAD[2*]
[1]Assistant Professor, Department of Mathematics ACS College of Engineering, Bengaluru, Karnataka.
[2]Professor, Department of Mathematics, Sri Krishnadevaraya University, Ananthapuram, Andhra Pradesh.
[1]lokeshmaths177@gmail.com,[2]rsprasad_racharla@yahoo.co.in

Abstract
In this paper we have considered the steady laminar flow of an visco-elastic electrically conducting Walter's-B fluid through a circular cylinder or pipe loosely packed with porous material subjected to uniform transverse magnetic field and taking Hall current into account. The entire flow domain without boundary layer approximations in the governing equations vis-a-vis, the fully developed solutions of the velocity and pressure drop are obtained and computationally discussed with reference to flow governing parameters. It is interesting to note that the elastic parameter reduces the fluid velocity nearly middle of the channel and then continuously boosting up throughout the cylinder. For engineering interest, we found skin friction analytically and computationally presented.
Keywords: Hall effects, steady flows, visco-elastic fluids, porous medium, circular cylinder.

1. Introduction:

Many researchers have analysed the solution by the method of successive approximation, taking the Newtonian solution as the initial solution following the method of Beard and Walters [3] which is valid only for small values of the elastic parameters. The study of flow through porous tubes or channels attracted many researchers in view of their applications in biomedical engineering, for example in the dialysis of blood in artificial kidneys, flow of blood in oxygenators, etc. Further, in many engineering applications such as the design of filters, the transpiration cooling, boundary layer control and the gaseous diffusion, the flow through porous tube finds numerous applications. The problem of flow through an annulus with porous walls has gained considerable importance in view of technological and aeronautical applications. Mishra and Roy [4] have studied the steady laminar flow of visco- elastic liquid through a pipe or cylinder with suction or injection. Yan and Finkel stein [5] have obtained the solution of laminar pipe flow with injection and suction through a porous wall. Juncu[6] studied heat/mass transfer from a circular cylinder with an internal heat/mass source in laminar cross flow at low Reynolds number. Cheng [7] has studied free convective heat and mass transfer from a horizontal cylinder of elliptic cross section in micro polar fluids. Opara[8] has investigated fluid instability between two rotating coaxial cylinders with radiative heat transfer. Esmaeilpouret al. [9] have applied He's method for laminar flow in a porous saturated pipe. Ganesan and Lokanath [10] have studied the effects of mass transfer and flow past a moving vertical cylinder with constant heat flux. Pattabhirana Charyulu[11] made a study on the flow through a circular pipe completely filled with porous material. Sharma et al. [12] obtained the numerical solution of steady motion of second order fluid past a circular cylinder with suction or injection. Sawchuk and Zamir [13] have investigated boundary layer on a circular cylinder in axial flow. Steady flow and heat transfer of a Sisko fluid in annular pipe was studied by Khan et al. [14]. Subramanyam et al. [15] have studied the unsteady laminar viscous conducting fluid through a circular cylinder bounded by permeable bed under the influence of exponentially decreasing pressure gradient. Laminar flow of a steady viscous incompressible fluid through a circular pipe under the influence of aligned magnetic field was discussed by Hughes and Young [16]. Saxena et al. [17] discussed the effect of MHD visco-elastic fluid flow, considering Rivlin-Ericksen model, through a circular cylinder bounded by a permeable bed. Recently, Munawar et al. [18] have investigated unsteady local non-similar boundary layer flow over a long slim cylinder. Ghasemi and Bayal [19] studied visco-elastic MHD flow and heat transfer of Walters'B fluid over a non-isothermal stretching sheet. Varshney et al. [20] have studied the effect of Hall current on MHD visco-elastic fluid flow through a circular cylinder embedded in a porous medium. Krishna and M.G. Reddy [22] discussed the unsteady MHD free convection in a boundary layer flow of an electrically conducting fluid through porous medium subject to uniform transverse magnetic field over a moving infinite vertical plate in the presence of heat source and chemical reaction. Krishna and G.S. Reddy [23] have investigated the simulation on the MHD forced convective flow through stumpy permeable porous medium (oil sands, sand) using Lattice Boltzmann method. Krishna and Jyothi [24] discussed the Hall effects on MHD Rotating flow of a visco-elastic fluid through a porous medium over an infinite oscillating porous plate with heat source and chemical reaction. Reddy et al.[25] investigated MHD flow of viscous incompressible nano-fluid through a saturating porous medium. Recently, Krishna et al. [26-29] discussed the MHD flows of an incompressible and electrically conducting fluid in planar channel. Veera Krishna et al. [30] discussed heat and mass transfer on unsteady MHD oscillatory flow of blood through porous arteriole. The effects of radiation and Hall current on an unsteady MHD free convective flow in a vertical channel filled with a porous medium have been studied by Veera Krishna et al. [31].

Keeping the above mentioned facts, in this paper we have considered the steady laminar flow of an elastic-viscous electrically conducting Walter's-B fluid through a circular cylinder or pipe loosely packed with porous material subjected to uniform transverse magnetic field and taking Hall current into account.

2. Formulation and Solution of the Problem:

Consider the steady laminar flow of an elastico-viscous electrically conducting (Walter's-B) fluid through a circular cylinder or pipe packed with porous material subjected to magnetic interaction and taking Hall current into account. The axis of the cylinder is taken along z-axis. The physical configuration of the problem is as shown in Fig.1. Cylindrical polar coordinates (r, θ, z) are used where r is measured from the axis of the cylinder, θ from some convenient meridian plane and z along the axis of the cylinder. The θ coordinate will not appear in our discussion due to axial symmetry, we have further assumed that a constant normal velocity of suction or injection is applied at the wall

$$u_r = u(r,z),\ u_\theta = 0,\ u_z = w(r,z) \tag{1}$$

$$u\frac{\partial u}{\partial r} + w\frac{\partial u}{\partial z} = -\frac{1}{\rho}\frac{\partial p}{\partial r} + \frac{1}{\rho}\left(\frac{\partial p^{1rr}}{\partial r} + \frac{\partial p^{1rz}}{\partial z}\right) - \frac{\sigma\beta_0 J_z}{\rho} - \frac{\eta_0}{\rho k}u \tag{2}$$

$$u\frac{\partial w}{\partial r} + w\frac{\partial w}{\partial z} = -\frac{1}{\rho}\frac{\partial p}{\partial z} + \frac{1}{\rho}\left(\frac{\partial p^{1rz}}{\partial r} + \frac{\partial p^{1zz}}{\partial z}\right) - \frac{\sigma\beta_0 J_x}{\rho} - \frac{\eta_0}{\rho k}w \tag{3}$$

When the strength of magnetic field is very large, the generalized Ohm's law is modified to include the Hall current so that,

$$J+\frac{\omega_e\tau_e}{H_0}J\times H=\sigma\left(E+\mu_e q\times H\right) \quad (4)$$

In Eq. (4), the electron pressure gradient, the ion-slip, and thermo-electric effects are neglected. We also assume that the electric field E=0 under assumptions reduces to

$$J_x-mJ_z=-\sigma\mu_e H_0 w=-\sigma B_0 w \quad (5)$$

$$J_z-mJ_x=-\sigma\mu_e H_0 u=-\sigma B_0 u \quad (6)$$

Where, $m=\omega_e\tau_e$ is the Hall parameter, on solving Eqs. (5) and (6), we obtain

$$J_x=\frac{\sigma B_0}{1+m^2}(um-w) \quad (7)$$

$$J_z=\frac{\sigma B_0}{1+m^2}(u+wm) \quad (8)$$

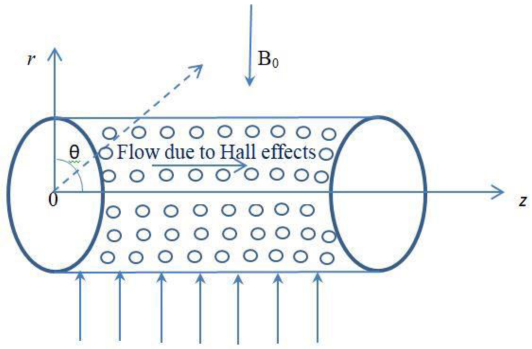

Fig. 1.Physical configuration of the problem

Using Eqs. (7) and (8), the equations of the motion with reference to the frame are given by

$$u\frac{\partial u}{\partial r}+w\frac{\partial u}{\partial z}=-\frac{1}{\rho}\frac{\partial p}{\partial r}+\frac{1}{\rho}\left(\frac{\partial p^{1rr}}{\partial r}+\frac{\partial p^{1rz}}{\partial z}\right)-\frac{\sigma\beta_0^2}{\rho\left(1+m^2\right)}(u+wm)-\frac{\eta_0}{\rho k}u \quad (9)$$

$$u\frac{\partial w}{\partial r}+w\frac{\partial w}{\partial z}=-\frac{1}{\rho}\frac{\partial p}{\partial z}+\frac{1}{\rho}\left(\frac{\partial p^{1rz}}{\partial r}+\frac{\partial p^{1zz}}{\partial z}\right)-\frac{\sigma\beta_0^2}{\rho\left(1+m^2\right)}(um-w)-\frac{\eta_0}{\rho k}w \quad (10)$$

Defining the non-dimensional parameter

$$\lambda=\frac{r}{a}(0\le\lambda\le 1) \quad (11)$$

The equations of continuity and momentum reduce to

$$\frac{1}{a^2}\frac{\partial u}{\partial\lambda}+\lambda\frac{\partial w}{\partial z}=0 \quad (12)$$

$$\frac{u}{a}\frac{\partial u}{\partial\lambda}+w\frac{\partial u}{\partial z}=\frac{1}{\rho}\frac{\partial p}{\partial r}+\nu\left[\frac{\partial^2 u}{\partial z^2}+\frac{1}{a^2}\frac{\partial^2 u}{\partial\lambda^2}+\frac{1}{a^2\lambda}\frac{\partial u}{\partial\lambda}-\frac{u}{a^2\lambda^2}\right]$$
$$-\frac{k_0}{\rho}[u\left(\frac{1}{a^3}\frac{\partial^3 u}{\partial\lambda^3}-\frac{\partial^3 w}{\partial z^3}+\frac{1}{a^2\lambda}\frac{\partial^2 w}{\partial\lambda\partial z}+\frac{1}{a^3\lambda}\frac{\partial^2 u}{\partial\lambda^2}+\frac{4u}{a^3\lambda^3}\right)$$
$$+w\left(\frac{\partial^3 u}{\partial z^3}-\frac{1}{a}\frac{\partial^3 w}{\partial\lambda\partial z^2}\right)$$
$$-\frac{6}{a^3}\frac{\partial u}{\partial\lambda}\frac{\partial^2 u}{\partial\lambda^2}-\frac{3}{a}\frac{\partial u}{\partial\lambda}\frac{\partial^2 u}{\partial\lambda\partial z}-\frac{1}{a^2}\frac{\partial u}{\partial z}\frac{\partial^2 w}{\partial\lambda^2}$$
$$+\frac{1}{a}\frac{\partial w}{\partial z}\frac{\partial^2 w}{\partial\lambda\partial z}-\frac{\partial w}{\partial z}\frac{\partial^2 u}{\partial z^2}-\frac{2}{a^2}\frac{\partial w}{\partial\lambda}\frac{\partial^2 u}{\partial\lambda\partial z}-\frac{2}{a^2}\frac{\partial u}{\partial\lambda}\frac{\partial^2 w}{\partial\lambda\partial z}-2\frac{\partial u}{\partial z}\frac{\partial^2 w}{\partial z^2}-\frac{1}{a^2}\frac{\partial u}{\partial z}\frac{\partial w}{\partial\lambda}$$
$$+\frac{1}{a\lambda}\left(\frac{\partial u}{\partial z}\right)^2-\frac{4}{a^3\lambda}\left(\frac{\partial u}{\partial\lambda}\right)^2]-\frac{\sigma\beta_0^2}{\rho\left(1+m^2\right)}(u-wm)-\frac{\eta_0}{\rho k}u \quad (13)$$

$$\frac{u}{a}\frac{\partial w}{\partial\lambda}+w\frac{\partial w}{\partial z}=-\frac{1}{\rho}\frac{\partial p}{\partial z}+\nu\left[\frac{\partial^2 w}{\partial z^2}+\frac{1}{a^2}\frac{\partial^2 w}{\partial\lambda^2}+\frac{1}{a^2\lambda}\frac{\partial w}{\partial\lambda}\right]$$
$$-\frac{k_0}{\rho}[u\left(\frac{1}{a^3}\frac{\partial^3 w}{\partial\lambda^3}+\frac{2}{a^3\lambda}\frac{\partial^2 w}{\partial\lambda^2}+\frac{1}{a}\frac{\partial^3 w}{\partial\lambda\partial z^2}-\frac{1}{a\lambda}\frac{\partial^2 w}{\partial z^2}\right)$$
$$-\frac{1}{a}\frac{\partial u}{\partial\lambda}\left(\frac{\partial^2 w}{\partial z^2}+\frac{1}{a^2}\frac{\partial^2 w}{\partial\lambda^2}+\frac{1}{a^2\lambda}\frac{\partial w}{\partial\lambda}\right)$$
$$-\frac{1}{a}\frac{\partial w}{\partial\lambda}\left(\frac{3}{a}\frac{\partial^2 w}{\partial\lambda\partial z}+\frac{\partial^2 u}{\partial z^2}+\frac{2}{a^2}\frac{\partial^2 u}{\partial\lambda^2}\right)$$
$$-\frac{\partial w}{\partial z}\left(\frac{2}{a}\frac{\partial^2 u}{\partial\lambda\partial z}+6\frac{\partial^2 w}{\partial z^2}+\frac{2}{a\lambda}\frac{\partial u}{\partial z}\right)\frac{\partial^2 w}{\partial z^2}$$
$$-\frac{2}{a}\frac{\partial u}{\partial z}\frac{\partial^2 w}{\partial\lambda\partial z}]-\frac{\sigma\beta_0^2}{\rho\left(1+m^2\right)}(um-w)-\frac{\eta_0}{\rho k}w$$

(14)

The boundary conditions are

$$u(\lambda,z)=0,\frac{\partial w}{\partial\lambda}=0 \quad \text{at} \quad \lambda=0 \quad (15)$$

$$w(\lambda,z)=0,(\lambda,z)=u_0 \quad \text{at} \quad \lambda=1 \quad (16)$$

2581-4575

International Journal For Recent Developments in Science & Technology

Crossref

A Peer Reviewed Research Journal

We now introduce a stream function ψ defined by

$$u(\lambda,z)=-\frac{1}{a\lambda}\frac{\partial\psi}{\partial z} \quad \text{and} \quad w(\lambda,z)=\frac{1}{a^2\lambda}\frac{\partial\psi}{\partial\lambda} \quad (17)$$

The function ψ satisfies the equation of continuity (12). We now write the stream function in the form of

$$\psi(\lambda,z)=\phi(\lambda)g(z) \quad (18)$$

Then the velocity components are given by

$$u(\lambda,z)=-\frac{1}{a\lambda}\phi(\lambda)\frac{\partial g}{\partial z} \quad \text{and} \quad w(\lambda,z)=\frac{1}{a^2\lambda}\frac{\partial\phi}{\partial\lambda}g(z) \quad (19)$$

Let $\bar{w}_0$ and $\bar{w}$ be the average velocity at z = 0 and local average velocity at some station z in the pipe respectively so that these are given by

$$\bar{w}_0=2\int_0^1 \lambda w(\lambda,0)d\lambda \quad (20)$$

and $\bar{w}=2\int_0^1 \lambda w(\lambda,z)\lambda d\lambda$ (21)

From the boundary condition (16) and the radial velocity component (17) one gets

$\frac{\partial g}{\partial z}=-\frac{au_0}{\phi(1)}$ and which on integration gives g(z)

$$=-\frac{au_0z}{\phi(1)}+A \quad (22)$$

Where, '*A*' is constant to be determined from the inlet conditions of the pipe.

Again from the boundary condition (15) and the expression (19)

$\phi(0)=0$, since $\frac{\partial g}{\partial z}$ is a non-zero constant with the help of (19) and (22) Eq.(18) gives

$$A=-\frac{a^2\bar{w}_0}{2\phi(1)} \quad (23)$$

Again from (22) and (23), we have

$$g(z)=-\frac{au_0z}{\phi(1)}+\frac{a^2\bar{w}_0}{2\phi(1)}=\frac{1}{\phi(1)}\left[\frac{1}{2}a^2\bar{w}_0-au_0z\right]$$

(24) Let

$$V(\lambda)=\frac{\frac{\partial\phi}{\partial\lambda}}{\lambda\phi(1)} \quad \text{and} \quad \bar{V}(\lambda)=\frac{\phi(\lambda)}{\lambda\phi(1)}=\frac{1}{\lambda}\int_0^1 tV(t)dt \quad (25)$$

Then, the velocity components (19) assume the following forms with the help of the Eqs. (22), (24) and (25)

$$u=u_0\bar{V}(\lambda) \quad (26)$$

$$w=\left(\frac{1}{2}\bar{w}_0-\frac{u_0z}{a}\right)V(\lambda) \quad (27)$$

Further, with the help of (18), (24) and (25), the stream function ψ can be put in the form of

$$\psi(\lambda,z)=\left(\frac{1}{2}a^2\bar{w}_0-au_0z\right)\lambda\bar{V}(\lambda) \quad (28)$$

In the equations *V* (λ) is some function of the distance parameter λ yet to be determined. We also note that since the suction or injection velocity is taken to be constant, the radial component of velocity becomes a function of λ only.

Substituting for u and w from (26) and (27) into the equations of motion (13) and (14) we get

$$-\frac{1}{\rho}\frac{\partial p}{\partial\lambda}=u_0^2\bar{V}\bar{V}'-\frac{\nu u_0}{a}\left[\bar{V}''+\frac{\bar{V}'}{\lambda}-\frac{\bar{V}}{\lambda^2}\right]$$
$$+\frac{K_0u_0^2}{a^2}\left[\bar{V}\bar{V}'''-\frac{1}{\lambda}\bar{V}V'+\frac{1}{\lambda}\bar{V}V''+\frac{4}{\lambda^3}\bar{V}^2-6\bar{V}\bar{V}''+VV'+2\bar{V}V'-\frac{4}{\lambda}\bar{V}'^2\right]$$
$$+\left(\frac{M^2}{1+m^2}+\frac{1}{K}\right)\bar{V} \quad (29)$$

$$-\frac{1}{\rho}\frac{\partial p}{\partial\lambda}=\left(\frac{1}{2}\bar{w}_0-\frac{u_0z}{a}\right)\left[\frac{u_0}{a}\left(\bar{V}V'-V^2\right)-\frac{\nu}{a^2}\left(V''+\frac{1}{\lambda}V'\right)\right.$$
$$\left.+\frac{K_0u_0}{a^3}\left(\bar{V}\bar{V}'''+\frac{2}{\lambda}\bar{V}V''-\frac{1}{\lambda}VV'-VV''-\bar{V}'V''+\frac{1}{\lambda}\bar{V}'V'+3V'^2-2V'\bar{V}''\right)\right]$$
$$+\left(\frac{M^2}{1+m^2}+\frac{1}{K}\right)RV \quad (30)$$

Differentiating Eq. (30) with respect to λ and eliminating p we get

$$R\left(\bar{V}'V'+\bar{V}'V''-2VV'\right)-\left(V'''+\frac{1}{\lambda}V''-\frac{1}{\lambda^2}V'\right)+RR_c\{\bar{V}'V^{iv}+5V'V''-VV'''-3\bar{V}''V''-2V'\bar{V}'''$$

$$+\frac{1}{\lambda}\left(2\bar{V}V''' - V'^2 - VV'' - \bar{V}''V' + \bar{V}'V''\right) + \frac{1}{\lambda^2}\left(VV' - 2\bar{V}V'' + \bar{V}'V'\right)\Big\} + \left(\frac{M^2}{1+m^2} + \frac{1}{K}\right)RV' = 0$$

(31)

The problem thus reduces to the solutions of a fourth order non-linear differential equations, If the elastic number Rc =0 we recover the corresponding equations for a Newtonian liquid. If there is no fluid suction or injection at the surface of the cylinder, then R =0 and Eq. (31) reduces to

$$V''' + \frac{1}{\lambda}V'' - \frac{1}{\lambda^2}V' = 0 \qquad (32)$$

The solution of (32) subject to the boundary conditions

$$V(1) = 0 = V'(0);\ \bar{V}(0) = 0,\ \bar{V}(1) = 1 \qquad (33)$$

Becomes a function V (λ) decreasing the well-known Poiseuille flow in a cylindrical pipe. This proves that the elastic elements in the viscous liquid play some role in the flow field only when there is suction or injection of the fluid on the surface of the cylinder. Thus, we can study the derivations from the Poiseuille flow by a perturbation method where the cross flow Reynolds number R is used as a perturbation parameter. The solution thus obtained will be valid for sufficiently small values of R. Making use of perturbation method, we expand the functions V (λ) and $\bar{V}$ (λ) in the forms

$$V(\lambda) = V_0(\lambda) + RV_1(\lambda) + R^2V_2(\lambda) + \ldots\ldots.. \qquad (34)$$

$$\bar{V}(\lambda) = \bar{V}_0(\lambda) + R\bar{V}_1(\lambda) + R^2\bar{V}_2(\lambda) + \ldots\ldots. \qquad (35)$$

Where

$$\bar{V}_\eta(\lambda) = \frac{1}{\lambda}\int_0^\lambda tV_\eta(t)\,dt \qquad (36)$$

And V_n and $\bar{V}_n$ are taken to be independent of R.

Inserting (34) and (35) into (29) and equating the coefficients of various powers of R to zero we get, Zeroth order approximation is

$$V_0''' + \frac{1}{\lambda}V_0'' - \frac{1}{\lambda^2}V_0' = 0 \qquad (37)$$

First order approximation is

$$V_1''' + \frac{1}{\lambda}V_1'' - \frac{1}{\lambda^2}V_1' = \bar{V}_0'V_0' + \bar{V}_0V_0'' - 2V_0V_0' + \left(\frac{M^2}{1+m^2} + \frac{1}{K}\right)V_0'$$

$$+Rc\Big[V_0V_0^{iv} + 5V_0'V_0'' - V_0V_0''' - 3\bar{V}_0'''V_0'' - 2V_0'\bar{V}_0'''$$

$$+\frac{1}{\lambda}\left(2\bar{V}_0V_0''' - V_0'^2 - V_0V_0'' - \bar{V}_0''V_0' + \bar{V}_0'V_0''\right)$$

$$+\frac{1}{\lambda^2}\left(V_0V_0' - 2\bar{V}_0V_0'' + \bar{V}_0'V_0'\right)\Big] + \left(\frac{M^2}{1+m^2} + \frac{1}{K}\right)V_0' \qquad (38)$$

Second order approximation is

$$V_2''' + \frac{1}{\lambda}V_2'' - \frac{1}{\lambda^2}V_2' = \bar{V}_0'V_1' + \bar{V}_1V_0' + \bar{V}_0V_1''$$

$$+\bar{V}_1V_0'' - 2\left(V_0V_1' + V_1V_0'\right) + \left(\frac{M^2}{1+m^2} + \frac{1}{K}\right)V_1'$$

$$+Rc\Big[\bar{V}_0V_1^{iv} + \bar{V}_1V_0^{iv} + 5\left(V_0'V_1'' + V_1'V_0''\right)$$

$$-\left(V_0V_1''' + V_1V_0'''\right) - 3\left(\bar{V}_0'''V_1'' + \bar{V}_1'''V_0''\right) - 2\left(V_0'\bar{V}_1''' + V_1'\bar{V}_0'''\right)$$

$$+\frac{1}{\lambda}\Big\{2\left(\bar{V}_0V_1''' + \bar{V}_1V_0'''\right) - 2V_0'V_1' - \left(V_0V_1'' + V_1V_0''\right)$$

$$-\left(\bar{V}_0''V_1' + \bar{V}_1''V_0'\right) + \left(\bar{V}_0'V_1'' + \bar{V}_1'V_0''\right)\Big\}$$

$$+\frac{1}{\lambda^2}\Big\{V_0V_1' + V_1V_0' - 2\left(\bar{V}_0V_1'' + \bar{V}_1V_0''\right) + \bar{V}_0'V_1' + \bar{V}_1'V_0'\Big\}\Big]$$

(39)

And so on

The conditions to be satisfied by V_n and $\bar{V}_n$ are

$$V_n(1) = V_n'(0) = 0 \quad \text{for } n = 0, 1, 2\ldots \qquad (40)$$

$$\bar{V}_0(1) = 1 \quad \text{and} \quad \bar{V}_n(1) = 0 \quad \text{for} \quad n \geq 1 \qquad (41)$$

It can be seen that the solutions of various order are

$$V_{(\lambda)}^{(0)} = -4(\lambda^2 - 1) \qquad (42)$$

$$\bar{V}_{(\lambda)}^{(0)} = -\lambda(\lambda^2 - 2) \qquad (43)$$

$$V_{(\lambda)}^{(1)} = -4(\lambda^2 - 1) + R\left(\frac{2}{9} - \lambda^2 + \lambda^4 - \frac{2}{9}\lambda^6\right)$$

$$+R\left(\frac{M^2}{1+m^2} + \frac{1}{K}\right)\left(\frac{1}{3}\lambda^2 - \frac{1}{4}\lambda^4 - \frac{1}{12}\right)$$

(44)

$$V_{(\lambda)}^{(1)} = -\lambda(\lambda^2-2) + R\left(\frac{1}{9}\lambda - \frac{1}{4}\lambda^3 + \frac{1}{6}\lambda^5 - \frac{1}{36}\lambda^7\right)$$
$$+R\left(\frac{M^2}{1+m^2}+\frac{1}{K}\right)\left(-\frac{1}{24}\lambda + \frac{1}{12}\lambda^3 - \frac{1}{24}\lambda^5\right)$$

(45)

$$V_{(\lambda)}^{(2)} = -4(\lambda^2-1) + R\left(\frac{2}{9} - \lambda^2 + \lambda^4 - \frac{2}{9}\lambda^6\right)$$
$$+R\left(\frac{M^2}{1+m^2}+\frac{1}{K}\right)\left(\frac{1}{3}\lambda^2 - \frac{1}{4}\lambda^4 - \frac{1}{12}\right)$$
$$+R^2\left[\left(\frac{83}{1350} - \frac{38}{135}\lambda^2 + \frac{11}{36}\lambda^4 - \frac{1}{9}\lambda^6 + \frac{1}{36}\lambda^8 - \frac{1}{450}\lambda^{10}\right)\right.$$
$$+\left(\frac{M^2}{1+m^2}+\frac{1}{K}\right)\left(-\frac{17}{540} - \frac{53}{360}\lambda^2 - \frac{1}{6}\lambda^4 + \frac{7}{108}\lambda^6 - \frac{1}{72}\lambda^8\right)$$
$$+R\left(\frac{M^2}{1+m^2}+\frac{1}{K}\right)^2\left(\frac{1}{288} - \frac{5}{288}\lambda^2 + \frac{1}{48}\lambda^4 - \frac{1}{144}\lambda^6\right)$$
$$\left.+Rc\left(-\frac{17}{45} + \frac{52}{45}\lambda^2 - \frac{8}{9}\lambda^6\right)\right] \qquad (46)$$

$$\bar{V}_{(\lambda)}^{(2)} = -\lambda(\lambda^2-2) + R\left(\frac{1}{9}\lambda - \frac{1}{4}\lambda^3 + \frac{1}{6}\lambda^5 - \frac{1}{36}\lambda^7\right)$$
$$+R\left(\frac{M^2}{1+m^2}+\frac{1}{K}\right)\left(-\frac{1}{24}\lambda + \frac{1}{12}\lambda^3 - \frac{1}{24}\lambda^5\right)$$
$$+R^2\left[\left(\frac{83}{2700}\lambda - \frac{19}{270}\lambda^3 + \frac{11}{216}\lambda^5 - \frac{1}{72}\lambda^7 + \frac{1}{360}\lambda^9 - \frac{1}{5400}\lambda^{11}\right)\right.$$
$$+\left(\frac{M^2}{1+m^2}+\frac{1}{K}\right)\left(-\frac{17}{1080}\lambda + \frac{53}{1440}\lambda^3 - \frac{1}{36}\lambda^5 + \frac{7}{864}\lambda^7 - \frac{1}{720}\lambda^9\right)$$
$$+\left(\frac{M^2}{1+m^2}+\frac{1}{K}\right)^2\left(\frac{2}{1152}\lambda - \frac{5}{1152}\lambda^3 + \frac{1}{288}\lambda^5 - \frac{1}{1152}\lambda^7\right)\sum_{i=1}^{n}(X_i-\bar{X})^2$$
$$\left.+Rc\left(-\frac{17}{90}\lambda + \frac{13}{45}\lambda^3 - \frac{1}{9}\lambda^7 + \frac{1}{90}\lambda^9\right)\right] \qquad (47)$$

From (26) and (25) with the help of (46) and (47) the expressions for the velocity components in the non-dimensional form are given by

$$\frac{u}{u_0} = -\lambda(\lambda^2-2) + R\left(\frac{1}{9}\lambda - \frac{1}{4}\lambda^3 + \frac{1}{6}\lambda^5 - \frac{1}{36}\lambda^7\right)$$
$$+R\left(\frac{M^2}{1+m^2}+\frac{1}{K}\right)\left(-\frac{1}{24}\lambda + \frac{1}{12}\lambda^3 - \frac{1}{24}\lambda^5\right)$$
$$+R^2\left[\left(\frac{83}{2700}\lambda - \frac{19}{270}\lambda^3 + \frac{11}{216}\lambda^5 - \frac{1}{72}\lambda^7 + \frac{1}{360}\lambda^9 - \frac{1}{5400}\lambda^{11}\right)\right.$$
$$+\left(\frac{M^2}{1+m^2}+\frac{1}{K}\right)\left(-\frac{17}{1080}\lambda + \frac{53}{1440}\lambda^3 - \frac{1}{36}\lambda^5 + \frac{7}{864}\lambda^7 - \frac{1}{720}\lambda^9\right)$$
$$+\left(\frac{M^2}{1+m^2}+\frac{1}{K}\right)^2\left(\frac{2}{1152}\lambda - \frac{5}{1152}\lambda^3 + \frac{1}{288}\lambda^5 - \frac{1}{1152}\lambda^7\right)$$
$$\left.+Rc\left(-\frac{17}{90}\lambda + \frac{13}{45}\lambda^3 - \frac{1}{9}\lambda^7 + \frac{1}{90}\lambda^9\right)\right]$$

(48)

$$\frac{w}{\bar{w}_0} = \left(\frac{1}{2} - \frac{R}{N_{\mathrm{Re}}}\frac{Z}{a}\right)\left[-4(\lambda^2-1) + R\left(\frac{2}{9} - \lambda^2 + \lambda^4 - \frac{2}{9}\lambda^6\right)\right.$$
$$+R\left(\frac{M^2}{1+m^2}+\frac{1}{K}\right)\left(\frac{1}{3}\lambda^2 - \frac{1}{4}\lambda^4 - \frac{1}{12}\right)$$
$$+R^2\left\{\left(\frac{83}{1350} - \frac{38}{135}\lambda^2 + \frac{11}{36}\lambda^4 - \frac{1}{9}\lambda^6 + \frac{1}{36}\lambda^8 - \frac{1}{450}\lambda^{10}\right)\right.$$
$$+\left(\frac{M^2}{1+m^2}+\frac{1}{K}\right)\left(-\frac{17}{540} - \frac{53}{360}\lambda^2 - \frac{1}{6}\lambda^4 + \frac{7}{108}\lambda^6 - \frac{1}{72}\lambda^8\right)$$
$$+\left(\frac{M^2}{1+m^2}+\frac{1}{K}\right)^2\left(\frac{1}{288} - \frac{5}{288}\lambda^2 + \frac{1}{48}\lambda^4 - \frac{1}{144}\lambda^6\right)$$
$$\left.\left.+Rc\left(-\frac{17}{45} + \frac{52}{45}\lambda^2 - \frac{8}{9}\lambda^6\right)\right\}\right] \qquad (49)$$

From Eq. (21) it can be shown that

$$\frac{w}{\bar{w}_0} = \left(1 - \frac{2R}{N_{\mathrm{Re}}}\frac{Z}{a}\right) \qquad (50)$$

Now, from Eqs. (47) and (48) we have

$$\frac{w}{\bar{w}} = \frac{1}{2}V_{(\lambda)}^{(2)} = -2(\lambda^2-1) + \frac{1}{2}R\left(\frac{2}{9} - \lambda^2 + \lambda^4 - \frac{2}{9}\lambda^6\right)$$
$$+\frac{1}{2}R\left(\frac{M^2}{1+m^2}+\frac{1}{K}\right)\left(\frac{1}{3}\lambda^2 - \frac{1}{4}\lambda^4 - \frac{1}{12}\right)$$

International Journal For Recent Developments in Science & Technology
2581-4575
Crossref
A Peer Reviewed Research Journal

$$+\frac{1}{2}R^2\left[\left(\frac{83}{1350}-\frac{38}{135}\lambda^2+\frac{11}{36}\lambda^4-\frac{1}{9}\lambda^6+\frac{1}{36}\lambda^8-\frac{1}{450}\lambda^{10}\right)\right.$$

$$+\left(\frac{M^2}{1+m^2}+\frac{1}{K}\right)\left(-\frac{17}{540}-\frac{53}{360}\lambda^2-\frac{1}{6}\lambda^4+\frac{7}{108}\lambda^6-\frac{1}{72}\lambda^8\right)$$

$$+\left(\frac{M^2}{1+m^2}+\frac{1}{K}\right)^2\left(\frac{1}{288}-\frac{5}{288}\lambda^2+\frac{1}{48}\lambda^4-\frac{1}{144}\lambda^6\right)$$

$$\left.+Rc\left(-\frac{17}{45}+\frac{52}{45}\lambda^2-\frac{8}{9}\lambda^6+\frac{1}{9}\lambda^8\right)\right] \quad (51)$$

From (29) and (30) we get pressure distribution as

$$\int_0^z \frac{\partial p}{\partial z}dz = p(\lambda,z)-p(\lambda,0)$$

(52)

$$\int_0^\lambda \frac{\partial p}{\partial \lambda}d\lambda = p(\lambda,z)-p(0,z)$$

(53)

From (52) and (53) it follows that

$$\int_0^z \frac{\partial p}{\partial z}dz+\left[\int_0^\lambda \frac{\partial p}{\partial \lambda}d\lambda\right]_{z=0} = p(\lambda,z)-p(0,0)$$

(54)

Where, $p(0,0)$ is the pressure at the entrance of the pipe on the axis. From (52), (30), (46) and (47) we have, the pressure drop in the axial direction is

$$\Delta P=\frac{Z}{a}\frac{1}{N_{\text{Re}}}\left(1-\frac{R}{N_{\text{Re}}}\frac{Z}{a}\right)\left[16-R\left\{12+(144\lambda^2-64)Rc+\left(2\lambda^2-\frac{2}{3}\right)\left(\frac{M^2}{1+m^2}+\frac{1}{K}\right)\right\}\right.$$

$$+R^2\left\{\frac{88}{135}-\frac{3}{10}\left(\frac{M^2}{1+m^2}+\frac{1}{K}\right)\right.$$

$$+\left(\frac{11}{72}-\frac{2}{3}\lambda^2+\frac{1}{2}\lambda^4\right)\left(\frac{M^2}{1+m^2}+\frac{1}{K}\right)^2$$

$$\left.\left.-\left(\frac{224}{15}+4\lambda^2-20\lambda^4+20\lambda^6\right)Rc-\frac{20}{23}Rc\left(\frac{M^2}{1+m^2}+\frac{1}{K}\right)\right\}\right]$$

(55)

The results hold for $|R|\le 1$. $\bar{V}_n(1)=0$ Positive values of R (or u_0) represent suction, while negative values represents injection at the wall. We may also deduce the solutions for the Newtonian fluid as particular cases from the above solution by taking $Rc = 0$.

The stress component

$$P^{'rz}=\frac{\eta_0}{a}\frac{\partial w}{\partial \lambda}-\frac{k_0}{a^2}\left[u\frac{\partial^2 w}{\partial \lambda^2}+aw\frac{\partial^2 w}{\partial \lambda \partial z}-2\frac{\partial u}{\partial \lambda}\frac{\partial w}{\partial \lambda}+\frac{u}{\lambda}\frac{\partial w}{\partial \lambda}\right]$$

(56)

The frictional force (Shear stress) is given by

$$\tau_0=-\frac{\left(P^{'rz}\right)_{\lambda=1}}{\rho v \bar{w}_0/a}=\left(\frac{1}{2}-\frac{R}{N_{\text{Re}}}\frac{Z}{a}\right)\left[-8+R\left\{\frac{2}{3}-\frac{1}{3}\left(\frac{M^2}{1+m^2}+\frac{1}{K}\right)\right\}\right.$$

$$+R^2\left\{\frac{26}{135}-\frac{17}{180}\left(\frac{M^2}{1+m^2}+\frac{1}{K}\right)+\frac{1}{144}\left(\frac{M^2}{1+m^2}+\frac{1}{K}\right)^2-\frac{32}{15}Rc\right\}\right]$$

$$+RRc\left\{32-\frac{16}{3}R-\frac{10}{3}\left(\frac{M^2}{1+m^2}+\frac{1}{K}\right)\right\}$$

(57)

From (28) and (47) the stream function in the non-dimensional form can be written as

$$\psi(\lambda,z)=\frac{\psi(\lambda,z)}{a^2\bar{w}_0}=\lambda\left(\frac{1}{2}-\frac{R}{N_{\text{Re}}}\frac{Z}{a}\right)\left[\lambda(2-\lambda^2)+R\left(\frac{1}{9}\lambda-\frac{1}{4}\lambda^3+\frac{1}{6}\lambda^5-\frac{1}{36}\lambda^7\right)\right.$$

$$+R\left(\frac{M^2}{1+m^2}+\frac{1}{K}\right)\left(-\frac{1}{24}\lambda+\frac{1}{12}\lambda^3-\frac{1}{24}\lambda^5\right)$$

$$+R^2\left[\left(\frac{83}{2800}\lambda-\frac{19}{270}\lambda^3+\frac{11}{216}\lambda^5-\frac{1}{72}\lambda^7+\frac{1}{360}\lambda^9-\frac{1}{5400}\lambda^{11}\right)\right.$$

$$+\left(\frac{M^2}{1+m^2}+\frac{1}{K}\right)\left(-\frac{17}{1080}\lambda+\frac{53}{1440}\lambda^3-\frac{1}{36}\lambda^5+\frac{7}{864}\lambda^7-\frac{1}{720}\lambda^9\right)$$

$$+\left(\frac{M^2}{1+m^2}+\frac{1}{K}\right)^2\left(\frac{2}{1152}\lambda-\frac{5}{1152}\lambda^3+\frac{1}{288}\lambda^5-\frac{1}{1152}\lambda^7\right)$$

$$\left.+Rc\left(-\frac{17}{90}\lambda+\frac{13}{45}\lambda^3-\frac{1}{9}\lambda^7+\frac{1}{90}\lambda^9\right)\right]$$

(58)

International Journal For Recent Developments in Science & Technology
2581-4575
Crossref
A Peer Reviewed Research Journal

3. Results and Discussion

The flow governed by the non-dimensional parameters namely viz. Hartman number (*M*), permeability parameter (*K*) , Hall parameter (*m*), Cross –flow Reynolds number (*R*), Elastic parameter (*Rc*), *Z/a* for the velocity and pressure drop. The profiles (2-7) depict for the velocity$w/\bar{w}_0$; (8 - 12) for the axial velocity $w/\bar{w}$; and (13 - 18) for the pressure drop while the other parameters being fixed. Table. 1 represents the frictional force with respect to all governing parameters and finally the Table. 2 has been shown the validation of the results. The Fig. 2 shows that the axial velocity reduces in the upper half of the channel with increasing Hartman number *M*, because of Lorentz force velocity continuously reduces throughout the cylinder. The magnitude of the velocity enhances with increasing porous parameter (*K*) and hall parameter (*m*) (Fig. 3 - 4). Lower the permeability lesser the fluid speed is observed in the entire fluid region. The axial velocity increases from the axis of the pipe to the wall during the flow, in the presence of the porous matrix sustains a retorting effect at all the sections whereas the elastic elements not have significant contributions . In the absence of elastic element and porous matrix the velocity attains higher in magnitude at every point of the cylinder. From Fig. 5, it is shown that when $R > 0$ the velocity reduces whereas $R < 0$ the velocity increases on nearly the upper half of the cylinder, and rest part of the channel is to increase throughout the cylinder. The Fig. 6 describes the variation of the velocity with elastic parameter. The magnitude of the velocity slightly decreases due to presence of elasticity. Particularly it is interesting to note that the elastic parameter reduces the fluid velocity nearly middle ($\lambda < 6$) of the channel and then continuously boosting up ($\lambda > 6$) throughout the cylinder. We also noticed that from the Fig. 7, an increasing *Z/a* leads to reduce the axial velocity in the flow of viscous fluid while the other parameter being fixed. The axial velocity distribution is obtained in the presence of fluid suction/injection at the surface of the cylinder. It is evident that from Eqn. (21) in the absence of cross flow (R = 0), axial velocity is given for $\frac{\omega}{\bar{\omega}_0} = 2(1-\lambda^2)$. This represents the flow in a solid pipe. It is noted from the Fig. 8 expression for maximum velocity occurs for $\lambda > 0$ with magnitude 2. It is quite interesting to note that at the centre of the cylinder, the velocity profiles intersect to each other. Thus it is concluded that flow is independent of cross flow at the centre line of the pipe. From the Fig. 8, it is also interesting to observe that a significant reduction of axial velocity due to resistive type Lorentz force, so it is evident that the axial velocity retorts with increasing the intensity of the magnetic field. The magnitude of the velocity enriches with increasing porous parameter *K* and Hall parameter *m* (Fig. 9 – 10). The axial velocity upsurges from the axis of the pipe to the wall during the flow in the presence of the porous matrix sustains a retarding effect at all the sections whereas the elastic elements not have significant contributions. In the absence of elastic element and porous matrix the velocity reaches higher in magnitude at every point of the cylinder. Fig. 11, evident that, the influence of suction parameter ($R > 0$) is to increase to half of the cylinder where as the reversal effect ($R < 0$) observed on the velocity in the upper half of the pipe, but injection fevers it, this is due to fact that hall current effect. The Fig. 12 conveys the variation of the velocity with elastic parameter. The magnitude of the velocity slightly diminishes due to presence of elasticity. Particularly it is interesting to note that the elastic parameter condenses the fluid velocity nearly middle ($\lambda < 6$) of the channel and then continuously boosting up ($\lambda > 6$) during the course of the cylinder. We also distinguished that from the Fig. 7, an increasing *Z/a* leads to

International Journal For Recent Developments in Science & Technology
2581-4575
Crossref
A Peer Reviewed Research Journal

reduce the axial velocity in the flow of viscous fluid while the other parameter being fixed. Fig. 13 exhibits the pressure variation for various values of Hartman numbers (*M*). The pressure drop enhances with increasing the intensity of magnetic field, it is also evident from the fact that in the presence of Hall current effect. It is observed that from the Fig. (14 - 15) the pressure distribution retards with increasing porosity parameter (*K*) and Hall parameter (*m*). It is also note that presence of porous matrix has no significant effect on pressure variation. It is evident from the Fig.16 that the injection contributes to reattain maximum pressure drop where as the reversal effect for increasing suction. We noticed that from the Fig. 17. The pressure variation increases with increasing elastic parameter throughout the cylinder. Likewise the pressure variation diminishes with increasing Z/*a* in entire pipe it is observed from the Fig. 18.

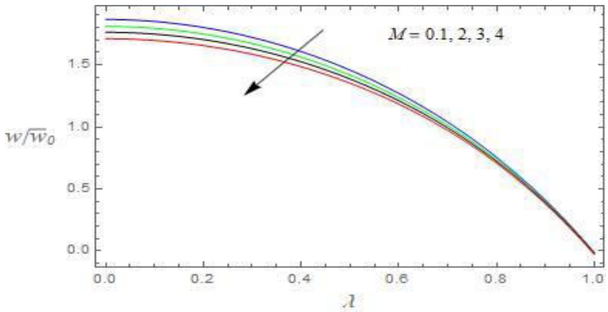

Fig. 2 The velocity profile against M with $K = 0.1,\ m = 1,\ R = 0.1,\ Rc = 50,\ Z/a = 20$

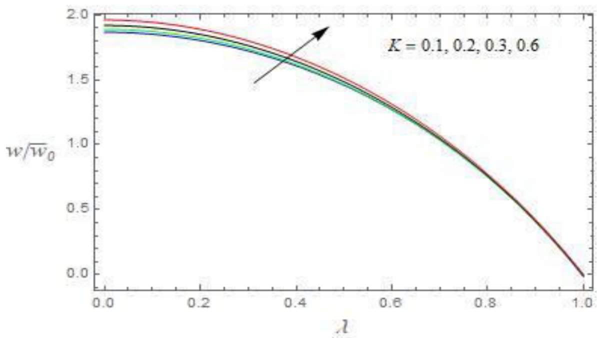

Fig. 3 The velocity profile against K with $M = 0.1,\ m = 1,\ R = 0.1,\ Rc = 50,\ Z/a = 20$

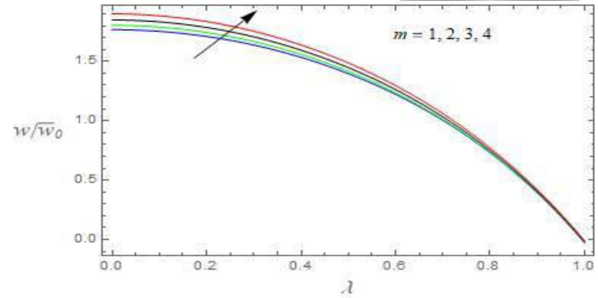

Fig. 4 The velocity profile against m with $M = 4,\ K = 0.1,\ R = 0.1,\ Rc = 50,\ Z/a = 20$

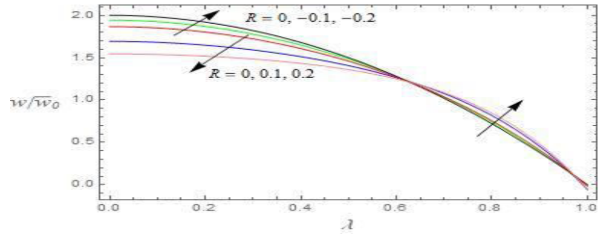

Fig. 5 The velocity profile against R with $M = 0.1,\ K = 0.1,\ m = 0.1,\ Rc = 50,\ Z/a = 20$

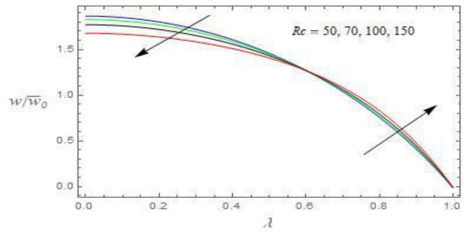

Fig. 6 The velocity profile against Rc with $M = 0.1,\ K = 0.1,\ m = 0.1,\ R = 0.1,\ Z/a = 20$

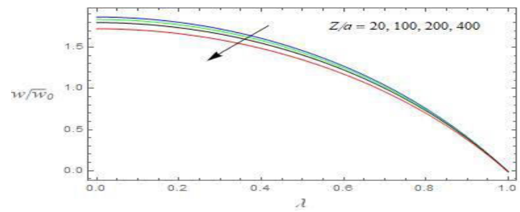

Fig. 7 The velocity profile against Z/a with $M = 0.1,\ K = 0.1,\ m = 0.1,\ R = 0.1,\ Rc = 50$

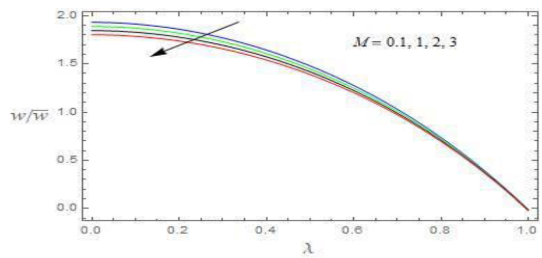

Fig. 8 The velocity profile against M with $K = 0.1,\ m = 1,\ R = 0.1,\ Rc = 20$

International Journal For Recent Developments in Science & Technology
2581-4575
Crossref
A Peer Reviewed Research Journal

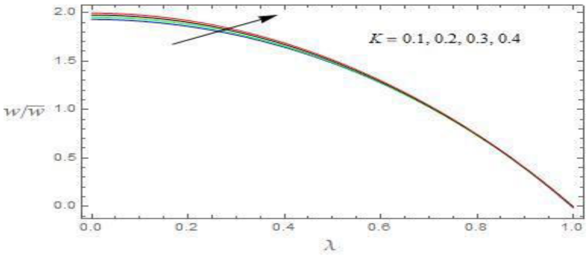

Fig. 9 The velocity profile against K with $M = 0.1,\ m = 1,\ R = 0.1,\ Rc = 20$

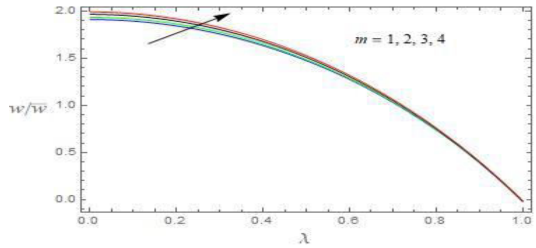

Fig. 10 The velocity profile against m with $M = 3,\ K = 0.1,\ R = 0.1,\ Rc = 20$

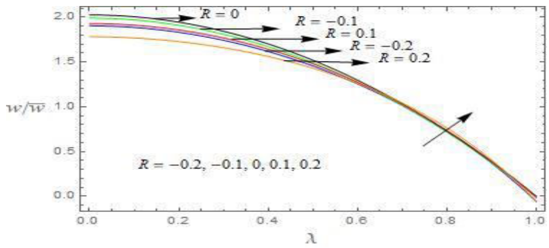

Fig. 11 The velocity profile against R with $M = 0.1,\ K = 0.1,\ m = 1,\ Rc = 20$

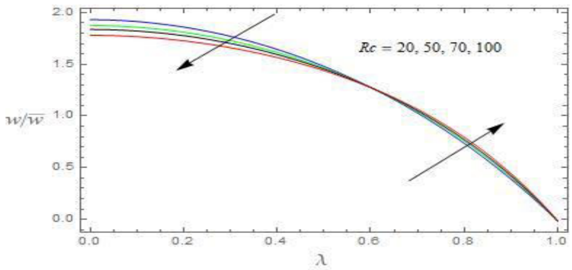

Fig. 12 The velocity profile against Rc with $M = 0.1,\ K = 0.1,\ m = 0.1,\ R = 0.1$

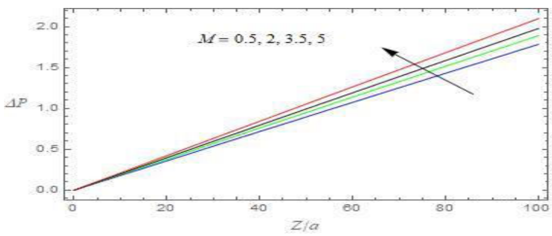

Fig. 13 The pressure profile against M with $K = 0.1,\ m = 1,\ R = 0.1,\ Rc = 0.1,\ \lambda = 0.1$

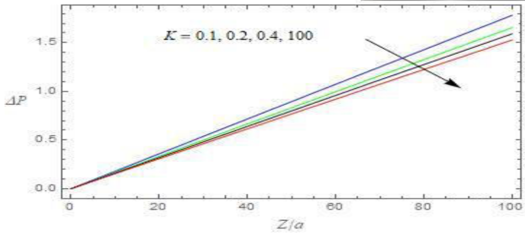

Fig. 14 The pressure profile against K with $M = 0.5,\ m = 1,\ R = 0.1,\ Rc = 0.1,\ \lambda = 0.1$

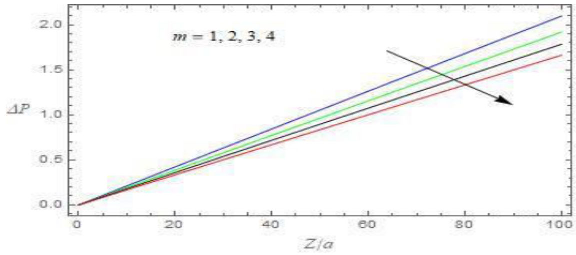

Fig. 15 The pressure profile against m with $M = 5,\ K = 0.1,\ R = 0.1,\ Rc = 0.1,\ \lambda = 0.1$

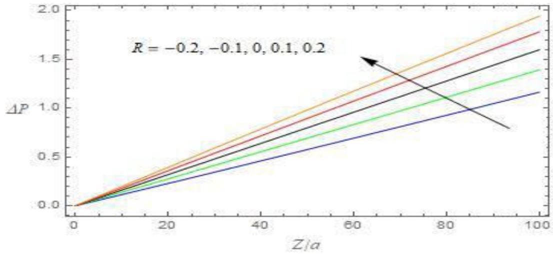

Fig. 16 The pressure profile against R with $M = 0.5,\ K = 0.1,\ m = 1,\ Rc = 0.1,\ \lambda = 0.1$

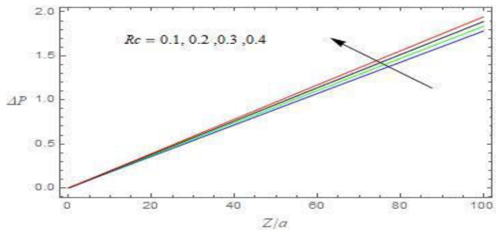

Fig. 17 The pressure profile against Rc with $M = 0.5,\ K = 0.1,\ m = 1,\ R = 0.1,\ \lambda = 0.1$

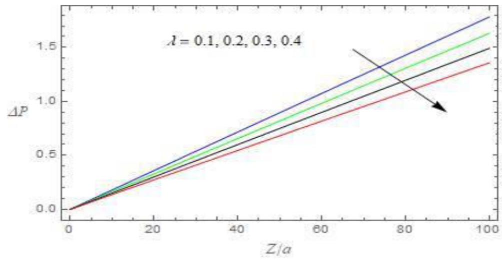

Fig. 18 The pressure profile against λ with $M = 0.5,\ K = 0.1,\ m = 1,\ R = 0.1,\ Rc = 0.1$

Table. 1 Skin friction

M	*K*	*M*	*R*	*Rc*	*z/a*	$-\tau_0$
0.5	**0.5**	**1**	**0.1**	**0.1**	**20**	3.66527
1						3.67036
1.5						3.67883
	1					3.65165
	1.5					3.64709
		2				3.66425
		3				3.66391
			0.2			3.32890
			0.3			2.99080
				0.2		3.34458
				0.3		3.02390
					50	3.64125
					100	3.60122

The effect of skin friction is an important aspect of the phenomena Table 1.displays the skin friction at various parameters of the flow through a pipe. All entries are negative and the absolute values of skin friction reduces with increasing poroucity parameter *K*, Hall parameter *m*, cross flow Reynolds number *R*, elastic parameter *Rc* and *Z/a* whereas increases the skin friction with increasing magnetic parameter *M* .Therefore we conclude that some amount of energy stored up as strain energy due to elastic parameter and suction reduce the shearing stress at the surface. It is a required outcome to avoid flow separation. Table. 2 represent the comparison of results for axial velocity distribution. We noticed that the results are excellent agreement with results of Barik et al. [21]

Table. 2 Comparison of axial velocity distribution at the surface of the cylinder.

$\lambda = 0.2;\ Z/a = 10;\ N_{Re} = 1000;$

M	*K*	*R*	*Rc*	Results of R.N. Barik [21]	Resultsof present study *m* = 0
0.5	0.1	0.1	0.1	1.87628	1.87627
1	0.2	0.2	0.2	1.86138	1.86136
1.5	0.3	0.3	0.3	1.83260	1.83261
2	0.4	0.4	0.4	1.78168	1.78169

4. Conclusions

We have considered the steady laminar flow of an elastic-viscous electrically conducting Walter's-B fluid through a circular cylinder or pipe loosely packed with porous material subjected to uniform transverse magnetic field and taking Hall current into account. The conclusions are made as the following.

1. The axial velocity reduces with increasing the intensity of the magnetic field.
2. Porosity parameter and Hall parameter increases the fluid velocity.
3. The magnitude of the velocity slightly decreases due to presence of elasticity.
4. Presence of magnetic field and porous matrix contribute slightly asymmetric flow with respect to centre of the pipe.
5. Elasticity and suction are counterproductive for experiencing greater skin friction and hence useful for controlling flow separation.

References:

[1]. K. Walters, The motion of elastico-viscous liquid contained between coaxial cylinders, Quart. J. Mech. Appl. Math. 13 (1960) 444–453.

[2]. K. Walters, The solution of flow problems in case of materials with memory, J. Mech. 1 (1962) 469–479.

[3]. D.W. Beard, K. Walters, Elastico-viscous boundary layer flows, two dimensional flow near a stagnation point, Proc. Camb. Phil. Soc. 60 (1964) 667–674.

[4]. S. Mishra, S. Roy, Steady laminar flow of elastic-viscous liquid through a pipe/cylinder with suction or injection, J. Appl. Phys.38 (5) (1967) 2072–2080.

[5]. S.W. Yuan, A.B. Flinkel Stein, Solution of Laminar pipe flow with injection and suction through a porous wall, Trans. A.C.Soc. Mech. Eng. 78 (1956) 719–724.

[6]. Gh.Juncu, Conjugate heat/mass transfer from a circular cylinder with an internal heat/mass source in laminar cross flow at low Reynolds numbers, Int. J. Heat Mass Transfer 48(2005) 419–424.

[7]. C.Y. Cheng, Free convection heat and mass transfer from a horizontal cylinder of elliptic cross section in micro polar fluids, Int. Commun. Heat Mass Transfer 33 (2006) 311–318.

[8]. F.E. Opara, Fluid instability between two rotating co-axial cylinders with radiative heat transfer, Astrophys. Space Sci. 43(1993) 197–204.

[9]. M. Esmaeilpour, D.D. Ganji, A.G. Davodi, N. Sadoughi, Application of He's method for laminar flow in a porous saturated pipe, Math. Mech. Appl. Sci. 33 (2010) 1112–1121.

[10]. P. Ganesan, P. Lokanath, Effects of mass transfer and flow pasta moving vertical cylinder with constant heat flux, Acta Mach.150 (2001) 179–190.

[11]. N.Ch. Pattabhirana Charyulu, Study on the flow through a circular pipe completely filled with porous material, Indian J. Pure. Appl. Math. 10 (6) (1979) 761.

[12]. H.G. Sharma, Manoj Kumar, U.M.A. Arora, Numerical solution of steady motion of second order fluid past a circular cylinder with suction or injection, in: Proc. of 30th CongressISTAM.IIT, New Delhi, 1985.

[13]. S.P. Sawchuk, M. Zamir, Boundary layer on a circular cylinder in axial flow, Int. J. Heat Flow 13 (1992) 184–188.

[14]. M. Khan, S. Munawar, S. Abbasbandy, Steady flow and heat transfer of a Sisko fluid to annular pipe, Int. J. Heat MassTransfer 53 (7–8) (2010) 1290–1297.

[15]. D. Subramanyam, G. Veera Raghava Reddy, N. Prabhakar Reddy, S.V.K. Verma, The unsteady laminar viscous conducting fluid through a circular cylinder bounded by permeable bed under the influence of exponentially decreasing pressure gradient, Acta Ciencia Indica XXXIIIM (3) (2007) 989–998.

[16]. W.F. Hughes, F.J. Young, Laminar flow of steady viscous incompressible fluid through a circular pipe under the influence of aligned magnetic field, Electro-magneto Dynamics of Fluids, John Wiley and Sons, New York, 1966, p. 254.

[17]. S.S. Saxena, G.K. Dubey, N.K. Varshney, Effect of MHD visco-elastic fluid and porous medium through circular cylinder bounded by a permeable bed, J. PAS Math. Sci. 15 (2009) 365–377.

[18]. S. Munawar, A. Mehmood, A. Ali, Unsteady local non-similar boundary layer flow over a long slim cylinder, Int. J. Phys. Sci. 6(34) (2011) 7709–7716.

[19]. E. Ghasemi, M. Bayal, Visco-elastic MHD flow of Walters B fluid and heat transfer over a non-isothermal stretching sheet, Int. J. Phys. Sci. 6 (21) (2011) 5022–5039.

[20]. N.K. Varshney, G.K. Sharma, J. Singh, Effect of hall currents on MHD visco-elastic fluid (Kuvshinshki) and porous medium through a circular cylinder bounded by a permeable bed, Int. J.Math. Arch. 2 (10) (2011) 2030–2035.

[21]. R.N.Barik, G.C.Dash, P.K.Rath, Steady laminar MHD flow of visco-elastic fluid through a porous pipe embedded in a porous medium, Alexandria Engineering Journal, vol. xx, pp. xx-xx, 2017.

[22]. M.Veera Krishna, M.Gangadhar Reddy, MHD Free Convective Boundary Layer Flow through Porous medium Past a Moving Vertical Plate with Heat Source and Chemical Reaction, Materials Today: Proceedings, vol. 5, pp. 91–98, 2018.

https://doi.org/10.1016/j.matpr.2017.11.058.

[23]. M.Veera Krishna, G.Subba Reddy, MHD Forced Convective flow of Non-Newtonian fluid through Stumpy Permeable Porous medium, Materials Today: Proceedings, vol. 5, pp. 175–183, 2018. https://doi.org/10.1016/j.matpr.2017.11.069.

[24]. M.Veera Krishna, Kamboji Jyotghi, Hall effects on MHD Rotating flow of a Visco-elastic Fluid through a Porous medium Over an Infinite Oscillating Porous Plate with Heat source and Chemical reaction, Materials Today: Proceedings, vol. 5, pp. 367–380, 2018. https://doi.org/10.1016/j.matpr.2017.11.094.

[25]. B. Siva Kumar Reddy, M. Veera Krishna , K.V.S.N. Rao, R. Bhuvana Vijaya, HAM Solutions on MHD flow of nano-fluid through saturated porous medium with Hall effects, Materials Today: Proceedings, vol. 5, pp. 120–131, 2018. https://doi.org/10.1016/j.matpr.2017.11.062.

[26]. VeeraKrishna.M and B.V.Swarnalathamma, Convective Heat and Mass Transfer on MHD Peristaltic Flow of Williamson Fluid with the Effect of Inclined Magnetic Field," AIP Conference Proceedings, vol. 1728, p. 020461, 2016. DOI: 10.1063/1.4946512

[27]. Swarnalathamma. B. V. and M. Veera Krishna, Peristaltic hemodynamic flow of couple stress fluid through a porous medium under the influence of magnetic field with slip effect AIP Conference Proceedings, vol. 1728, p. 020603, 2016. DOI: 10.1063/1.4946654.

[28]. VeeraKrishna.M and M.Gangadhar Reddy, MHD free convective rotating flow of Visco-elastic fluid past an infinite vertical oscillating porous plate with chemical reaction, IOP Conf. Series: Materials Science and Engineering, vol. 149, p. 012217, 2016 DOI: 10.1088/1757-899X/149/1/012217.

[29]. VeeraKrishna.M and G.Subba Reddy, Unsteady MHD convective flow of Second grade fluid through a porous medium in a Rotating parallel plate channel with temperature dependent source, IOP Conf. Series: Materials Science and Engineering, vol. 149, p. 012216, 2016. DOI: 10.1088/1757-899X/149/1/012216.

[30]. Veera Krishna.M., B.V.Swarnalathamma and J. Prakash, "Heat and mass transfer on unsteady MHD Oscillatory flow of blood through porous arteriole, Applications of Fluid Dynamics, Lecture Notes in Mechanical Engineering, vol. XXII, pp. 207-224, 2018. Doi: 10.1007/978-981-10-5329-0_14.

[31]. M.Veera Krishna, G.Subba Reddy, A.J.Chamkha, "Hall effects on unsteady MHD oscillatory free convective flow of second grade fluid through porous medium between two vertical plates," Physics of Fluids, vol. **30**, 023106 (2018); doi: 10.1063/1.5010863